Letters

Quasi-Y-Source Boost DC–DC Converter

Yam P. Siwakoti, Frede Blaabjerg, and Poh Chiang Loh

***Abstract*—In this letter, a new topology called "quasi-Y-source dc–dc converter" is presented. It inherits all the advantages of the original Y-source converter. In addition, the new topology draws a continuous current from the source, which is definitely more appropriate for most renewable sources. It also has dc-current-blocking capacitors, which will definitely help to prevent the coupled inductor core from saturation. Experimental testing has proven the validity of the proposed network and its application as a high boost dc–dc converter.**

***Index Terms*—Coupled inductor, dc-ac inverter, dc-dc converter, impedance source network, Y-source network, Z-source network.**

I. Introduction

THE design of front-end and/or intermediate step-up dc–dc converter with a continuous input current and wide range of voltage gain is one of the most challenging requirements faced by many distributed power generation and conditioning systems. It is especially true when intermittent sources like fuel cells, photovoltaic panels, and wind turbines are used [1], [2]. To meet this challenging requirement, various impedance networks have been developed to provide an efficient means of converting power with a wide range of voltage gain. Improvements to the impedance networks by introducing coupled magnetics have also been lately proposed for achieving even higher voltage boosting, while using a shorter shoot-through time [4]. They include the Γ-source [5], T-source [6], trans-Z-source [7], TZ-source [8], LCCT-Z-source [9], high-frequency-transformer-isolated [10], and Y-source [11] networks. Among them, the Y-source network is more versatile and can in fact be viewed as the generic network, from which the Γ-source, T-source, and trans-Z-source networks are derived. It is, therefore, a high-gain network with more generic winding design flexibility for the coupled magnetics.

The Y-source network has earlier been tested as a dc–dc converter, whose schematic is shown in Fig. 1(a) [12]. Its gain has indeed been proven higher than other classical impedance networks even with a smaller shoot-through duty cycle used. Its current drawn from the source is, however, discontinuous or pulsating between zero and a finite value, which is certainly not appropriate for most renewable sources. A simple modification to smoothen the current is presented in [9] by using an additional input capacitor with the T-source or trans-Z-source network. The same technique can be applied to the Y-source network like shown in Fig. 1(b). The modified network can indeed draw a continuous input current, but only when certain capacitance ratio between C_1 and C_2 is accurately set, and parasitic resistances minimized as much as possible. The modified network can also face the risk of large inrush current at startup and can face input oscillation caused by input parasitic inductances and capacitances C_1 and C_2. Another approach for smoothing the input current should thus be considered, which [13] and [14] have recommended using an additional input inductor and a capacitor. These additional components, when used with the Y-source network, lead to the modified dc–dc converter shown in Fig. 1(c). Although having an inductor in series with the source will definitely prevent any step-change in current, the modified network in Fig. 1(c) will undesirably face higher voltage stresses across its components, as shown later in the letter.

A third current smoothing technique, which overcomes the above concerns, is thus proposed in this letter for implementing the new quasi-Y-source boost converter shown in Fig. 1(d). The proposed converter is again a high-voltage boost converter implemented with high-frequency magnetics, but with a continuous input current drawn from the source. It is capable of handling a wide range of input voltage, while not increasing voltage stresses sustained by its components. The proposed converter is thus more suitable for renewable power conditioning systems. In addition, its two capacitors are placed such that they block dc current from flowing through the coupled inductor, and hence preventing its core from saturation. Operational principles and mathematical derivations of the new converter topology are presented in Section II, before showing its experimental results in Section III. Findings drawn are finally concluded in Section IV.

II. Principles of Operation

Fig. 1(a) and (d) shows the Y-source dc–dc converter [11] and proposed quasi-Y-source dc–dc converter. Both converters use the same coupled inductor with three windings (N_1, N_2, N_3) and capacitor C_1, whose positions in the converters are kept unchanged. The proposed converter, however, uses an additional dc-blocking capacitor C_2 in series with N_1 and an input inductor L_{In} in series with the source. Its diode D_1 has also been moved to between negative terminal of C_2 and drain of active switch SW. Despite these changes, both Y-source converters in

Manuscript received March 5, 2015; revised April 30, 2015; accepted May 30, 2015. Date of publication June 3, 2015; date of current version August 21, 2015.

The authors are with the Department of Energy Technology, Aalborg University, Aalborg 9220, Denmark (e-mail: yas@et.aau.dk; fbl@et.aau.dk; pcl@et.aau.dk).

Color versions of one or more of the figures in this paper are available online at http://ieeexplore.ieee.org.

Digital Object Identifier 10.1109/TPEL.2015.2440781

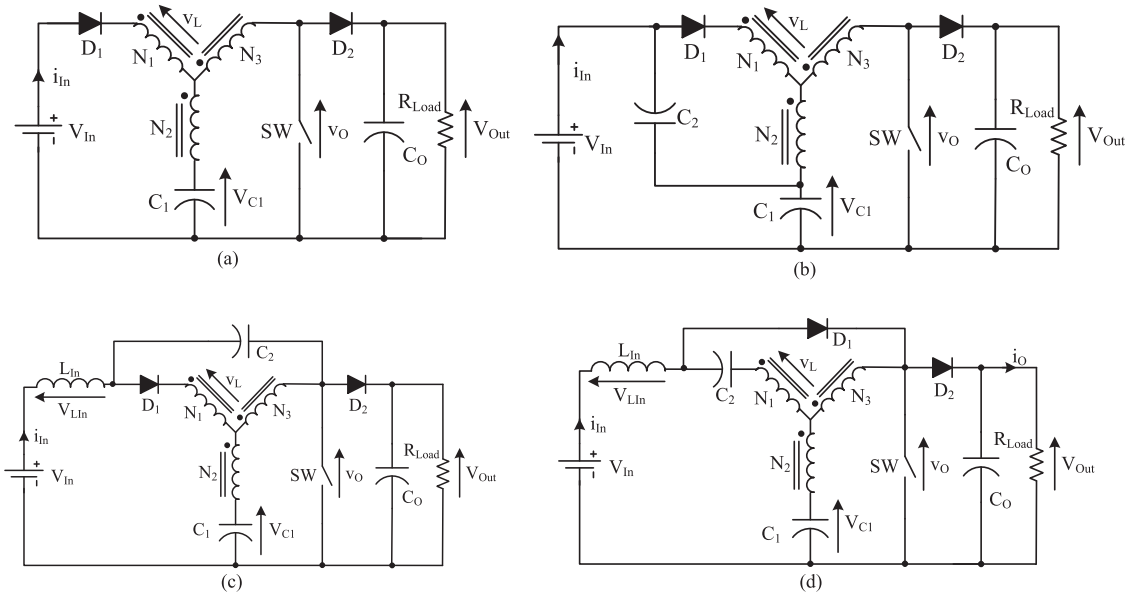

Fig. 1. Y-source dc–dc converters (a) without input current smoothing, and with input current smoothing based on (b) [9], (c) [13], [14], and (d) the proposed technique.

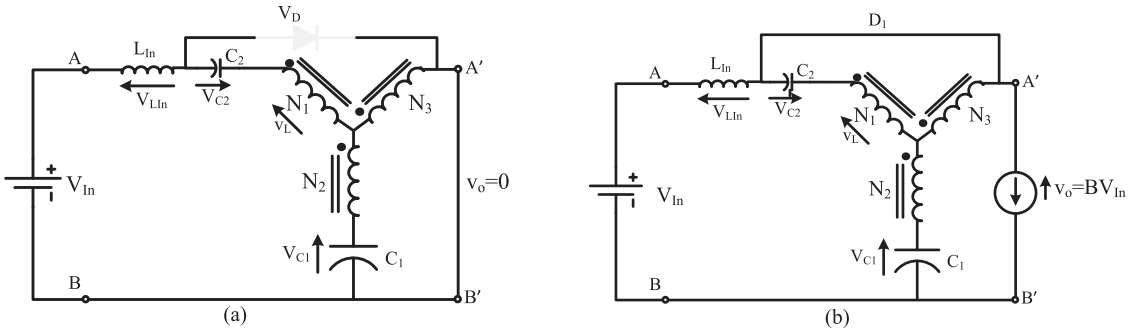

Fig. 2. Equivalent circuits of quasi-Y-source converter when in (a) shoot-through and (b) non-shoot-through states.

Fig. 1(a) and (d) produce two operating states, named respectively as the shoot-through and non-shoot-through states. The former corresponds to turning ON SW with D_1 reverse-biased naturally like in Fig. 2(a). Relevant circuit expressions for this state can then be written like in (1) and (2), whereN_1, N_2 and N_3 are the winding turns of the coupled inductor

$$V_{C1} + \frac{N_2}{N_1} v_L - \frac{N_3}{N_1} v_L = 0 \Rightarrow v_L = \frac{N_1}{N_3 - N_2} V_{C1} \quad (1)$$

$$V_{\mathrm{In}} - v_{L_{\mathrm{In}}} + V_{C2} - v_L - \frac{N_2}{N_1} v_L - V_{C1} = 0 \Rightarrow v_{L_{\mathrm{In}}} = V_{\mathrm{In}} + V_{C2} - V_{C1} - \left(\frac{N_1 + N_2}{N_1} \right) v_L. \quad (2)$$

By next turning OFF SW to initiate the non-shoot-through state, the equivalent circuit changes to that shown in Fig. 2(b). During this state, D_1 is also forced to conduct, which when analyzed, leads to those circuit expressions given in (3)–(5)

$$V_{C2} - v_L - \frac{N_3}{N_1} v_L = 0 \Rightarrow v_L = \frac{N_1}{N_1 + N_3} V_{C2} \quad (3)$$

$$v_{L_{\mathrm{In}}} = V_{\mathrm{In}} + V_{C2} - V_{C1} - \left(\frac{N_1 + N_2}{N_1} \right) v_L \quad (4)$$

$$V_{\mathrm{In}} - v_{L_{\mathrm{In}}} - v_o = 0 \Rightarrow v_O = V_{C1} - V_{C2} + \left(\frac{N_1 + N_2}{N_1} \right) v_L. \quad (5)$$

State-space averaging, when performed with (1) and (3), then results in (6) for computing voltage ratio across C_1 and C_2. This ratio can obviously be changed by varying d_{ST}, which represents duty ratio or fractional on-time of SW in a switching period

$$\left(\frac{N_1}{N_3 - N_2} V_{C1} \right) d_{\mathrm{ST}} + \left(\frac{N_1}{N_1 + N_3} V_{C2} \right) (1 - d_{\mathrm{ST}}) = 0 \Rightarrow \frac{V_{C2}}{V_{C1}} = \frac{N_1 + N_3}{N_2 - N_3} \frac{d_{\mathrm{ST}}}{1 - d_{\mathrm{ST}}}. \quad (6)$$

Repeating state-space averaging again with (2) and (4) results in (7), which together with (6) allows expressions for the individual capacitor voltages to be derived, as given in (8)

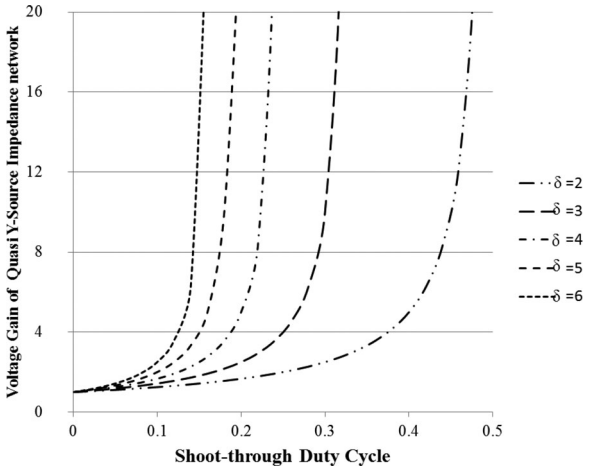

Fig. 3. Theoretical voltage gain G_v of the quasi-Y-source network obtained with different duty cycle $d_{\rm ST}$ and coupled-inductor winding factor δ.

and (9)

$$\left\{V_{\rm In}+V_{C2}-V_{C1}-\left(\frac{N_1+N_2}{N_1}\right)v_L\right\}d_{\rm ST} + \left\{V_{\rm In}+V_{C2}-V_{C1}-\left(\frac{N_1+N_2}{N_1}\right)v_L\right\} \times(1-d_{\rm ST})=0 \Rightarrow V_{C2}=V_{C1}-V_{\rm In} \quad (7)$$

$$V_{C2}=\frac{\frac{N_1+N_3}{N_2-N_3}d_{\rm ST}V_{\rm In}}{1-\frac{N_1+N_2}{N_2-N_3}d_{\rm ST}} \quad (8)$$

$$V_{C1}=\frac{(1-d_{\rm ST})V_{\rm In}}{1-\frac{N_1+N_2}{N_2-N_3}d_{\rm ST}}. \quad (9)$$

Now, using (3), (5), (8), and (9), the peak value $\hat{v}_O$ of the network output voltage v_O during the non-shoot-through state can be determined as (10), from which the network voltage gain $G_v=\hat{v}_O/V_{\rm In}$ can be determined in terms of winding factor δ of the coupled inductor and boost factor B of the quasi-Y-source impedance network. More specifically, δ and B are defined as $\delta=\frac{N_1+N_2}{N_2-N_3}$ and $B=\frac{1}{1-\delta d_{\rm ST}}$, respectively

$$\hat{v}_O=\frac{1}{1-\frac{N_1+N_2}{N_2-N_3}d_{\rm ST}}V_{\rm In}=\frac{1}{1-\delta d_{\rm ST}}V_{\rm In}=BV_{\rm In}. \quad (10)$$

From the denominator of (10), the range of variation for $d_{\rm ST}$ can further be determined as

$$0\le d_{\rm ST}<d_{\rm ST,max}=1/\delta. \quad (11)$$

Comparing (10) with its companion expression derived in [11] for the Y-source network also reveals that winding factors for the Y-source and proposed quasi-Y-source converters are different. More specifically, winding factor of the Y-Source impedance network is determined as $K=\frac{N_1+N_3}{N_3-N_2}$, while winding factor of the proposed quasi-Y-source network is determined as $\delta=\frac{N_1+N_2}{N_2-N_3}$. Despite that, voltage gains generated by both networks are the same so long as their winding factors are set equal ($K=\delta$). Like the Y-source network, voltage gain of the quasi-Y-source network can therefore also be set equal ($\delta=2$) or higher ($\delta>2$) than that of the Z-source network [3]. This possibility is demonstrated in Fig. 3 for different δ. For each considered δ, different $N_1:N_2:N_3$ ratios are also available for realizing it, which are collectively summarized in Table I. These winding ratios must however satisfy the inequalities of $1<N_2$ and $N_2>N_3$, which are different from those of $1<N_3$ and $N_3>N_2$ derived in [11] for the Y-source network. The proposed quasi-Y-source impedance network, however, has the advantage of drawing continuous current from the source, which the Y-source network cannot achieve. Moreover, capacitors C_1 and C_2 help to block dc current from the coupled-inductor, and hence preventing its core from saturation. These two features make the topology well suited for renewable power generation.

TABLE I
GAIN OF QUASI-Y-SOURCE IMPEDANCE NETWORK REALIZED WITH DIFFERENT WINDING FACTOR (δ) AND TURNS RATIO (N_1:N_2:N_3)

$\delta=\frac{N_1+N_2}{N_2-N_3}$	$d_{\rm ST,max}$	Gain G_v	$N_1:N_2:N_3$
2	1/2	$(1-2d_{\rm ST})^{-1}$	(1:3:1), (2:4:1), (3:5:1)
3	1/3	$(1-3d_{\rm ST})^{-1}$	(1:2:1), (3:3:1), (2:4:2)
4	1/4	$(1-4d_{\rm ST})^{-1}$	(2:2:1), (1:3:2), (5:3:1)
5	1/5	$(1-5d_{\rm ST})^{-1}$	(3:2:1), (2:3:2), (1:4:3)
6	1/6	$(1-6d_{\rm ST})^{-1}$	(4:2:1), (3:3:2), (2:4:3)

Regarding the two capacitor C_1 and C_2, their voltage ratings should also be chosen based on (6), (8), and (9), while their capacitances should be chosen based on (12). Derivation of (12) is based on determining current expressions for the capacitors in each state, and then performing state-space averaging using them. The derivation is slightly lengthy and hence not shown in this letter

$$C_1=(\delta-1)C_2. \quad (12)$$

It should, in addition, be mentioned that the above equations derived for the network have assumed continuous conduction mode, where diode D_1 in Fig. 2(b) will always conduct. This may not be true when the load, switching frequency and/or input inductance $L_{\rm In}$ is small. A new discontinuous conduction mode may, in turn, be created when current through D_1 in Fig. 2(b) eventually falls to zero, before the next shoot-through state is triggered. The same discontinuous mode has also been experienced by the first Z-source network proposed, which according to [15] can be avoided by enforcing a minimum network inductance. For the quasi-Y-source network, it means choosing input inductance $L_{\rm In}$ to be higher than the minimum value computed with (13). Derivation of (13) is, however, not included to keep the letter concise

$$L_{\rm In\_min}=\frac{\delta V_{\rm Out}}{2f_sI_{\rm in}}(1-d_{\rm ST})d_{\rm ST} \quad (13)$$

where f_s, $I_{\rm in}$, and $V_{\rm Out}$ represent the switching frequency, average input current, and nearly constant output voltage of the converter, respectively.

TABLE II
COMPARISON OF Y-SOURCE DC–DC CONVERTERS SHOWN IN FIG. 1

Parameter for Comparison	Original Y-Source	Modified Topologies with Continuous Input Currents		
		Y-Source with Existing Current Smoothing Techniques		Proposed Quasi-Y-Source
	Fig. 1(a)	Fig. 1(b)	Fig. 1(c)	Fig. 1(d)
$G_v = V_{Out}/V_{In}$	$\frac{1}{1-Kd_{ST}}$	$\frac{1}{1-Kd_{ST}}$	$\frac{1}{1-(1+K)d_{ST}}$	$\frac{1}{1-\delta d_{ST}}$
V_{C1}	$(1-d_{ST})G_vV_{In}$	$(1-d_{ST})G_vV_{In}$	$(1-d_{ST})G_vV_{In}$	$(1-d_{ST})G_vV_{In}$
V_{C2}	NA	$Kd_{ST}G_vV_{In}$	$Kd_{ST}G_vV_{In}$	$(\delta-1)d_{ST}G_vV_{In}$
V_{D1}	$(K-1)G_vV_{In}$	$(K-1)G_vV_{In}$	$(1+K)G_vV_{In}$	$(\delta-1)G_vV_{In}$
$0 < d_{ST} < d_{ST,max}$	$0 \le d_{ST} < \frac{1}{K}$	$0 \le d_{ST} < \frac{1}{K}$	$0 \le d_{ST} < \frac{1}{1+K}$	$0 \le d_{ST} < \frac{1}{\delta}$
Features	• Very high voltage gain. • Versatile. • Discontinuous input current.	• Very high voltage gain. • Versatile. • Continuous input current • High inrush current. • Very sensitive to ESR of capacitor and parameter variations. • Unwanted resonance due to parasitic.	• Very high voltage gain. • Versatile. • Continuous input current • Higher voltage stress on components.	• Very high voltage gain. • Versatile. • Continuous input current • No inrush current. • Stress on components remains same as of original Y-source network.

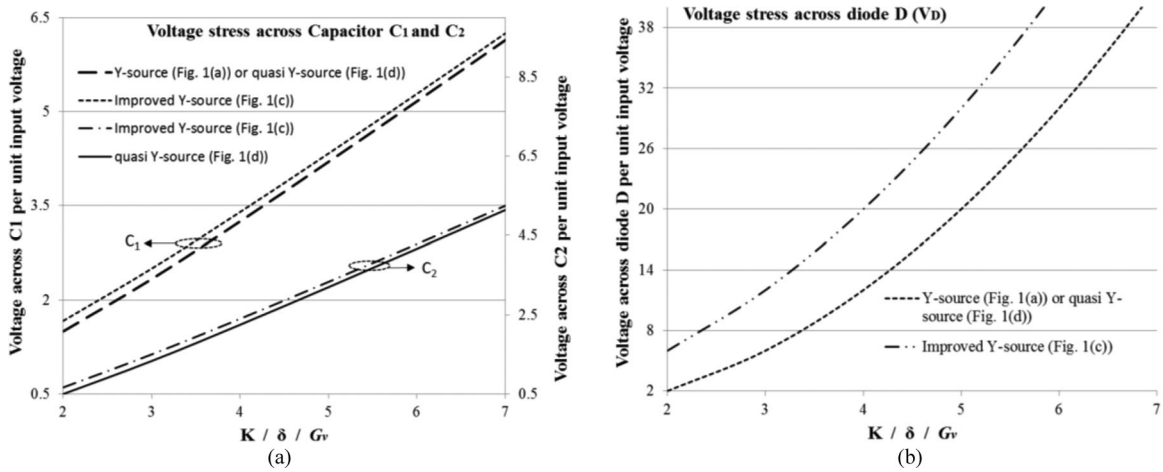

Fig. 4. Comparison of voltage stresses across (a) capacitors C_1 and C_2, and (b) diode D_1 of converters shown in Fig. 1 when operated with same voltage gain G_v and winding factor $K = \delta$.

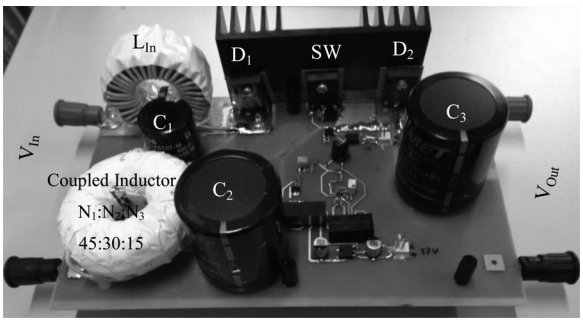

Fig. 5. Experimental 300-W quasi-Y-source dc–dc converter with $\delta = 5$ ($N_1 : N_2 : N_3 = 3 : 2 : 1 = 45 : 30 : 15$).

TABLE III
EXPERIMENTAL COMPONENTS AND PARAMETERS

Parameter/Description	Value
Power rating (P)	300 W
Input voltage (V_{In})	50 V
Output voltage (V_{Out})	200 V
DC-blocking capacitors	$C_1 = 470\ \mu$F, 400-V *Kemet*
	$C_2 = 150\ \mu$F, 400-V *Kemet*
Input Inductor (L_{In})	1.5 mH
Output buffer capacitor (C_3)	470 μF, 400-V *Kemet*
Switching frequency (f_s)	24.41 kHz
Shoot-through duty cycle(d_{ST})	0.15
Winding factor (δ)	5
Turns ratio ($N_1 : N_2 : N_3$)	45:30:15 on C055710A2 core
Switch SW	C2M0080120D
Diode D_1	C3D25170H
Diode D_2	C3D20060D

Similar mathematical derivations for gain and stress have also been performed on the two converters shown in Fig. 1(b) and (c), whose continuous input currents are obtained based on techniques discussed in [9], [13], and [14]. The derived expressions are summarized in Table II for comparison, where it can clearly be seen that voltage stresses experienced by components in Fig. 1(b) are the same as those of the original Y-source network shown in Fig. 1(a) if the same voltage gain and winding factor are set for both converters. The converter in Fig. 1(b), however, experiences some limitations previously summarized in Section I, which are again mentioned in Table II for comprehensiveness.

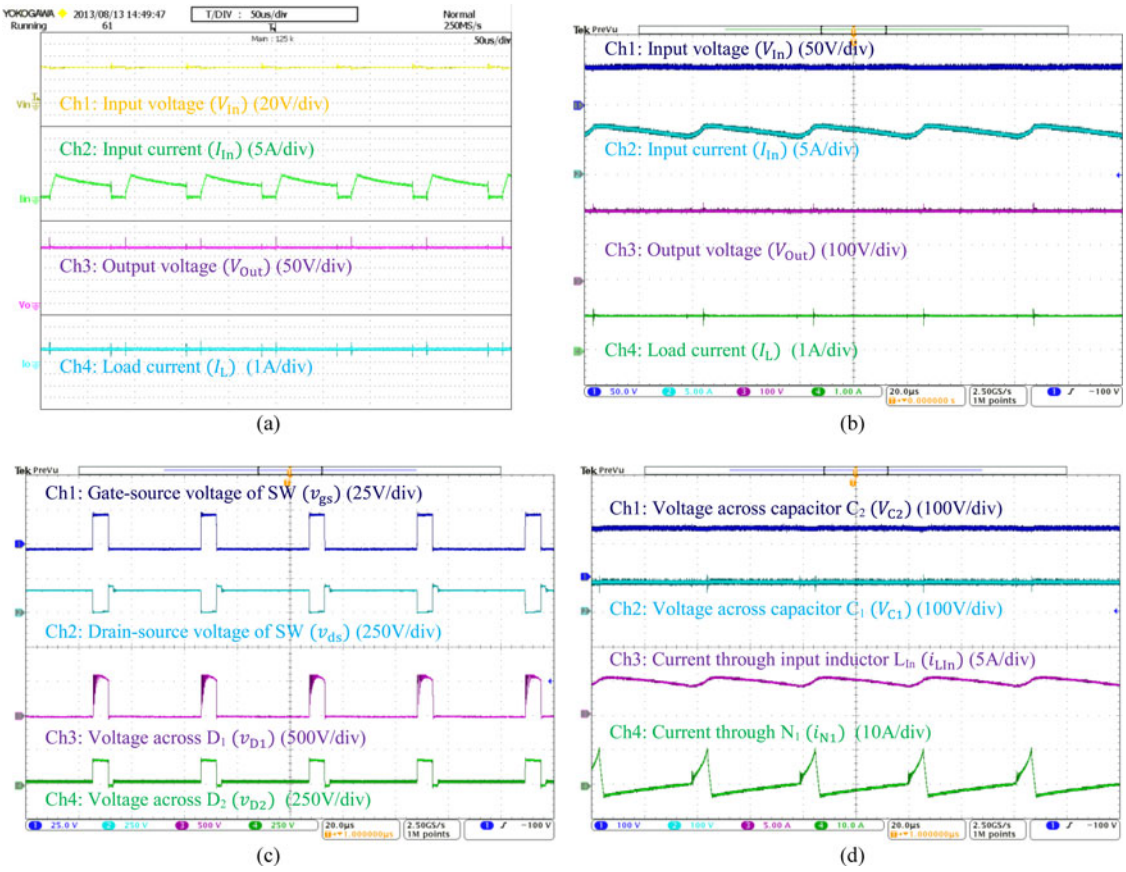

Fig. 6. Experimental waveforms of (a) original Y-source dc–dc converter in Fig. 1(a) with $d_{\mathrm{ST}} = 0.1875$, $K = 4$, and $f_s = 12.6\,\mathrm{KHz}$, and (b)–(d) quasi-Y-source dc–dc converter with $d_{\mathrm{ST}} = 0.1875$, $\delta = 5$, and $f_s = 24.4\,\mathrm{KHz}$.

In contrast, voltage stresses experienced by components of the converter shown in Fig. 1(c) is higher than the Y-source converter shown in Fig. 1(a) even when the same voltage gain and winding factor are used for both converters. This can be seen in Fig. 4, where voltage stresses of capacitors C_1 and C_2, and diode D_1 are plotted. Stresses of other components like switch SW and diode D_2 are not shown since they are the same for all converters shown in Fig. 1. In particular, for the converter shown in Fig. 1(c), its voltage stress across D_1 in Fig. 4 is noted to be much higher, which should hence be avoided where possible. To summarize, converters modified with existing current smoothing techniques shown in Fig. 1(b) and (c) are generally not comparable with the proposed quasi-Y-source converter because of its unique features mentioned earlier in the section and summarized in Table II.

III. Experimental Results and Discussions

A prototype has been built in the laboratory for verifying the performances of the proposed converter. Layout of the converter is shown in Fig. 5, while its parameters are summarized in Table III. Among the listed parameters, $\delta = 5$ can be substituted to (11) for computing the shoot-through range as $0 \leq d_{\mathrm{ST}} < 1/5$. The chosen d_{ST} of 0.15 in Table III is thus a valid value, which, when used, will give rise to a computed gain of 4 according to (10). This gain is the same as that of the original Y-source converter when the same d_{ST} and winding factor $K = 5$ are used. The output voltage of the proposed converter will, hence, be boosted to $V_{\mathrm{Out}} = 200$ V if its input voltage is set to 50 V. This computed output voltage is indeed the same as that read from the third experimental trace shown in Fig. 6(b). The converter is also noted to draw continuous current from the source, as seen from the second trace shown in Fig. 6(b). This is definitely different from the pulsating input current drawn by the original Y-source network, as seen from the second trace plotted in Fig. 6(a).

The proposed topology with its continuous input current and high voltage boost is, therefore, more suitable for renewable and distributed power generation. Its output voltage and current are also relatively constant and stable, as seen from the third and fourth traces shown in Fig. 6(b). Its interfacing with external loads will, therefore, not cause unexpected complications. Other waveforms showing component voltages and currents measured from the experimental prototype are given in Fig. 6(c) and (d). In particular, the fourth trace in Fig. 6(d) shows the current through winding N_1 centering along the horizontal zero-axis. This is expected because of the dc-blocking feature of C_2, which is connected in series with N_1. Other measured amplitudes in Fig. 6(c) and (d) have also been noted to be in agreement with theoretical values calculated using expressions derived in Section II, which

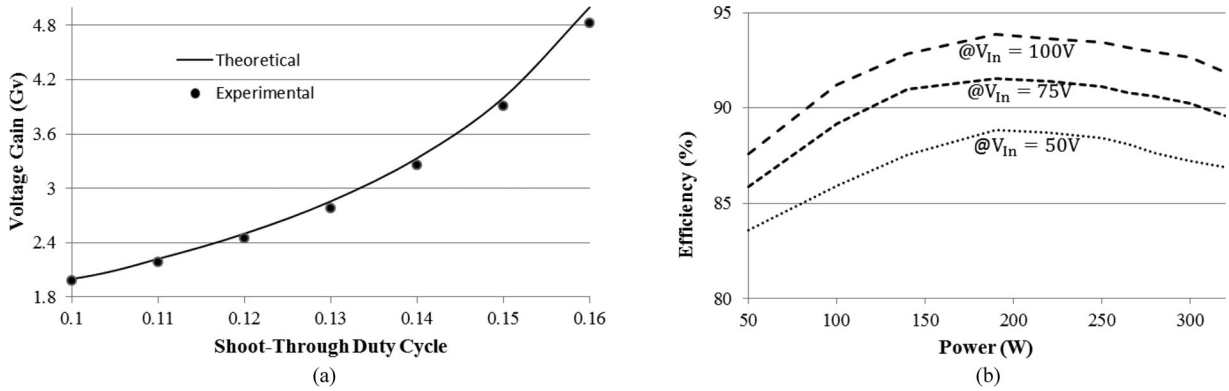

Fig. 7. Measured (a) voltage gain and (b) efficiency of the quasi-Y-source dc–dc converter.

to a great extent have verified performances expected from the network.

To further demonstrate its parasitic sensitivity (caused by resistances and/or leakage inductances of the coupled magnetics [16]) and efficiency, Fig. 7(a) and (b) has been plotted. Fig. 7(a) shows the measured and computed voltage gains of the converter at different shoot-through duty ratios. As expected, parasitic influences have caused the two gains to become more different at a higher shoot-through duty ratio. On the other hand, Fig. 7(b) shows the converter efficiency at different duty cycles, input voltages, and output powers, while keeping its output voltage regulated at 200 V. The figure clearly shows efficiency of the quasi-Y-source converter being slightly lower than that of the Y-source converter [12]. This is expected since the quasi-Y-source converter uses additional input components $L_{\rm In}$ and C_2, which carry high currents when in the boost mode.

The maximum efficiency of the quasi-Y-source converter has also been read as 93.9% at 10% duty ratio when the load is 200 W. It falls to 88% at the same load when the duty ratio is raised to 15%. This drop in efficiency at a high shoot-through duty cycle is presently a concern faced by all impedance-source converters. Its cause is mainly due to the flow of large shoot-through current, whose loss contribution can be reduced by using better graded wires for the coupled magnetics and busbars for the converter on the printed circuit board. Upon resolving these issues, power through the converter will be raised to match the switch chosen and capacity expected from a typical renewable source tied to the grid.

IV. Conclusion

This letter proposes a new quasi-Y-source boost dc–dc converter, which inherits all advantages from the existing Y-source dc–dc converter. The inherited features include a very high-voltage boost and flexibility in designing its winding magnetics. The new topology will, in addition, draw a continuous input current that better suits most renewable sources. Its two dc-current blocking capacitors will also help to prevent saturation of the coupled inductor. Mathematical derivations and experimental results for verification have clearly demonstrated the expected performances and, hence, practicality of the proposed dc–dc converter.

References

[1] F. Blaabjerg, R. Teodorescu, Z. Chen, and M. Liserre, "Power converters and control of renewable energy systems," presented at the Int. Conf. Power Electron.2004, Pusan, Korea, Oct. 2004.

[2] Q. Zhao and F. C. Lee, "High-efficiency, high step-up DC–DC converters," *IEEE Trans. Power Electron.*, vol. 18, no. 1, pp. 65–73, Jan. 2003.

[3] F. Z. Peng, "Z-source inverter," in *Proc. Ind. Appl. Conf.*, Oct. 13–18, 2002, vol. 2, pp. 775–781.

[4] Y. P. Siwakoti, F. Z. Peng, F. Blaabjerg, P. C. Loh and G. E. Town, "Impedance Source network for electric power conversion—Part I: A topological review" *IEEE Trans. Power Electron.*, vol. 30, no. 2, pp. 699–716, Feb. 2015.

[5] P. C. Loh, D. Li, and F. Blaabjerg, "Γ-Z-source inverters," *IEEE Trans. Power Electron.*, vol. 28, no. 11, pp. 4880–4884, Nov. 2013.

[6] R. Strzelecki, M. Adamowicz, N. Strzelecka and W. Bury, "New type t-source inverter," in *Proc. Compat. Power Electron.*, May 2009, pp. 191–195.

[7] W. Qian, F. Z. Peng and H. Cha, "Trans-Z-source inverters," *IEEE Trans. Power Electron.*, vol. 26, no. 12, pp. 3453–3463, Dec. 2011.

[8] M. K. Nguyen, Y. C. Lim. and Y. G. Kim, "TZ-source inverters," *IEEE Trans. Ind. Electron.*, vol. 60, no. 12, pp. 5686–5695, Dec. 2013.

[9] M. Adamowicz, R. Strzelecki, F. Z. Peng, J. Guzinski, and H. A. Rub, "New type LCCT-Z-source inverters," in *Proc.14th Eur. Conf. Power Electron. Appl.*, Sep. 2011, pp. 1–10.

[10] S. Jiang, D. Cao, and F. Z. Peng, "High frequency transformer isolated z-source inverters," in *Proc. Appl. Power Electron. Conf.*, Mar. 2011, pp. 442–449.

[11] Y. P. Siwakoti, P. C. Loh, F. Blaabjerg, and G. Town, "Y-source impedance network," *IEEE Trans. Power Electron.*, vol. 29, no. 7, pp. 3250–3254, Jul. 2014.

[12] Y. P. Siwakoti, P. C. Loh, F. Blaabjerg, S. J. Andreasen, and G. E. Town, "Y-source impedance network based boost DC/DC converter for distributed generation," *IEEE Trans. Ind. Electron.*, vol. 62, no. 2, pp. 1059–1069, Feb. 2015.

[13] W. Mo, P. C. Loh, and F. Blaabjerg, "Asymmetrical Γ-source inverters," *IEEE Trans. Ind. Electron.*, vol. 61, no. 2, pp. 637–647, Feb. 2014.

[14] M. K. Nguyen, Y. C. Lim, and S. J. Park, "Improved trans-z-source inverter with continuous input current and boost inversion capability," *IEEE Trans. Power Electron.*, vol. 28, no. 10, pp. 4500–4510, Oct. 2013.

[15] M. Shen and F. Z. Peng, "Operation modes and characteristics of the z-source inverter with small inductance or low power factor," *IEEE Trans. Ind. Electron.*, vol. 55, no. 1, pp. 89–96, Jan. 2008.

[16] Y. P. Siwakoti, P. C. Loh, F. Blaabjerg, and G. E. Town, "Effects of leakage inductances on magnetically-coupled impedance-source networks" *IEEE Trans. Power Electron.*, vol. 29, no. 11, pp. 5662–5666, Nov. 2014.